PLOS | ONE

RESEARCH ARTICLE

A novel mechanism of "metal gel-shift" by histidine-rich Ni^{2+}-binding Hpn protein from *Helicobacter pylori* strain SS1

Rahul Mahadev Shelake[1], **Yuki Ito**[1], **Junya Masumoto**[1], **Eugene Hayato Morita**[2,3], **Hidenori Hayashi**[1]*

1 Proteo-Science Center, Ehime University, Matsuyama, Japan, **2** Laboratory of Molecular Cell Physiology, Faculty of Agriculture, Ehime University, Matsuyama, Japan, **3** Department of Chemistry, Faculty of Science, Josai University, Saitama, Japan

* hayashi.hidenori.mj@ehime-u.ac.jp

Citation: Shelake RM, Ito Y, Masumoto J, Morita EH, Hayashi H (2017) A novel mechanism of "metal gel-shift" by histidine-rich Ni^{2+}-binding Hpn protein from *Helicobacter pylori* strain SS1. PLoS ONE 12(2): e0172182. doi:10.1371/journal.pone.0172182

Editor: Elena A. Rozhkova, Argonne National Laboratory, UNITED STATES

Received: October 26, 2016

Accepted: January 31, 2017

Published: February 16, 2017

Data Availability Statement: All relevant data are within the paper and its Supporting Information files.

Funding: The authors received no specific funding for this work.

Competing interests: The authors have declared that no competing interests exist.

Abstract

Sodium dodecyl sulphate-polyacrylamide gel electrophoresis (SDS-PAGE) is a universally used method for determining approximate molecular weight (MW) in protein research. Migration of protein that does not correlate with formula MW, termed "gel shifting" appears to be common for histidine-rich proteins but not yet studied in detail. We investigated "gel shifting" in Ni^{2+}-binding histidine-rich Hpn protein cloned from *Helicobacter pylori* strain SS1. Our data demonstrate two important factors determining "gel shifting" of Hpn, polyacrylamide-gel concentration and metal binding. Higher polyacrylamide-gel concentrations resulted in faster Hpn migration. Irrespective of polyacrylamide-gel concentration, preserved Hpn-Ni^{2+} complex migrated faster (3–4 kDa) than apo-Hpn, phenomenon termed "metal gel-shift" demonstrating an intimate link between Ni^{2+} binding and "gel shifting". To examine this discrepancy, eluted samples from corresponding spots on SDS-gel were analyzed by matrix-assisted laser desorption/ionization-time-of-flight mass spectrometry (MALDI-TOF-MS). The MW of all samples was the same (6945.66±0.34 Da) and identical to formula MW with or without added mass of Ni^{2+}. MALDI-TOF-MS of Ni^{2+}-treated Hpn revealed that monomer bound up to six Ni^{2+} ions non-cooperatively, and equilibrium between protein-metal species was reliant on Ni^{2+} availability. This corroborates with gradually increased heterogeneity of apo-Hpn band followed by compact "metal-gel shift" band on SDS-PAGE. In view of presented data metal-binding and "metal-gel shift" models are discussed.

Introduction

The major human pathogen *Helicobacter pylori*, responsible for severe gastric diseases including intestinal ulcers and adenocarcinoma, requires two key Ni-containing enzymes (urease and hydrogenase) for survival in acidic gastrointestinal conditions [1]. Thus, *H. pylori* produce unique Ni^{2+}-binding histidine-rich proteins required in the maturation of urease and hydrogenase. One of the first candidates involved in Ni^{2+} homeostasis in *H. pylori* was isolated and named Hpn (*Helicobacter pylori* protein binding to nickel) [2]. Hpn contains 28 histidine residues (46.7%) with two stretches of repeated histidines at positions 11–17 and 28–33 (**Fig 1A**). It also contains two short repeating motifs (EEGCC) in the internal part positioned at 38–42 and 51–55. The relative affinity of Hpn towards divalent metal ions was found to be different under *in vivo* and *in vitro* conditions indicating the complex nature of the protein [2–5]. Initial Hpn mutation studies in *H*. *pylori* showed that the mutant strain was more sensitive to Ni^{2+} than a wild-type strain [2,6,7]. Inductively coupled plasma-mass spectrometry and equilibrium dialysis studies revealed that average five Ni^{2+} ions (5.1±0.2) bind to Hpn in a pH-dependant manner and forms a range of multimeric complexes (>500, 136, 55, 34, 26, 20, 14 and 7 kDa) in solution that exists in equilibrium depending on buffer content [3,4]. The pH titration and competition experiments using EDTA confirmed that the metal-binding to Hpn is a reversible process [3–5]. Even though some amino-acid residues vital for metal-binding were identified [8–10], distribution of metal-binding sites and equilibrium between protein-metal species in Hpn is not yet known. Hpn may act in Ni^{2+} storage as a 'reservoir' or in channelizing Ni^{2+} to other proteins [3,4,11].

Even though sodium dodecyl sulfate-polyacrylamide gel electrophoresis (SDS-PAGE) is the most commonly used method for the determination of approximate MW of proteins; unusual electrophoretic behavior in SDS-PAGE has been reported for Hpn, making its identification problematic [3]. This phenomenon of unpredictable migration rate on SDS-PAGE against actual formula MW of protein is termed "gel shift" (not to be confused with the electrophoretic mobility shift assay for protein-DNA interactions). The "gel shifting" has also been reported for several other histidine-rich proteins including Hpn **(Table 1)** [3,7,12–18] as well as different helical membrane proteins [19–21] including some isobaric peptides (peptides with the same MW) from various organisms [22]. HspA from *Helicobacter*, which has a unique C-terminus containing a histidine-rich region, also exhibited a higher MW of 15.5 kDa than the expected 13 kDa [23] indicating that the "gel shift" behavior might be attributable to histidine-rich region. However, the molecular mechanism is yet to be clarified. Six possible mechanisms responsible for "gel shifting" of a protein have been hypothesized in previous reports: (a) divergent higher order (secondary or tertiary) structure; (b) difference in Stokes-Einstein (hydrodynamic) radius of the protein-surfactant complex; (c) variation in the intrinsic net charge of the protein; (d) number of bound SDS molecules; (e) post-translational modifications; or (f) binding of cofactors such as metal ions to the protein [19–21,24–26]. Nevertheless, polyacrylamide-gel concentration can dictate magnitude and direction of some proteins in SDS-gel [27].

Recently, attempts have been made to investigate these molecular mechanisms using segments of various membrane proteins, and the findings indicated that there might be no single universal mechanism that accounts for the anomalous migration of all proteins. In fact, each protein or class of proteins may have unique chemistry responsible for "gel shifting" behavior. It is an interesting question that whether "gel shifting" in Hpn is linked to the displacement of protein-protein, protein-metal, and/or protein-SDS interactions, but these need further investigation.

We cloned the *hpn* gene from the Sydney Strain 1 (SS1) of *H*. *pylori*, a standardized mouse model [28]. Our preliminary data demonstrated the altered migratory position for Hpn on SDS-PAGE when Hpn was expressed in Ni^{2+}-supplied medium suggesting role of Ni^{2+} in altered migration. We find that the migration rate of Ni^{2+}-treated Hpn on SDS-PAGE was altered because of preserved protein-metal complexes. Some SDS-resistant protein-protein interactions (**supporting information, Table A in S1 File**) and protein-metal complexes (**supporting information, Table B in S1 File**) can also preserve in electrophoretic separation upon SDS-PAGE provided interaction is stronger [29–31]. Also, many studies reported that the "reconstructive" denaturation can retain some protein-metal complexes on SDS-PAGE but altered migration is not generally observed except for some Ca^{2+}-binding proteins such as

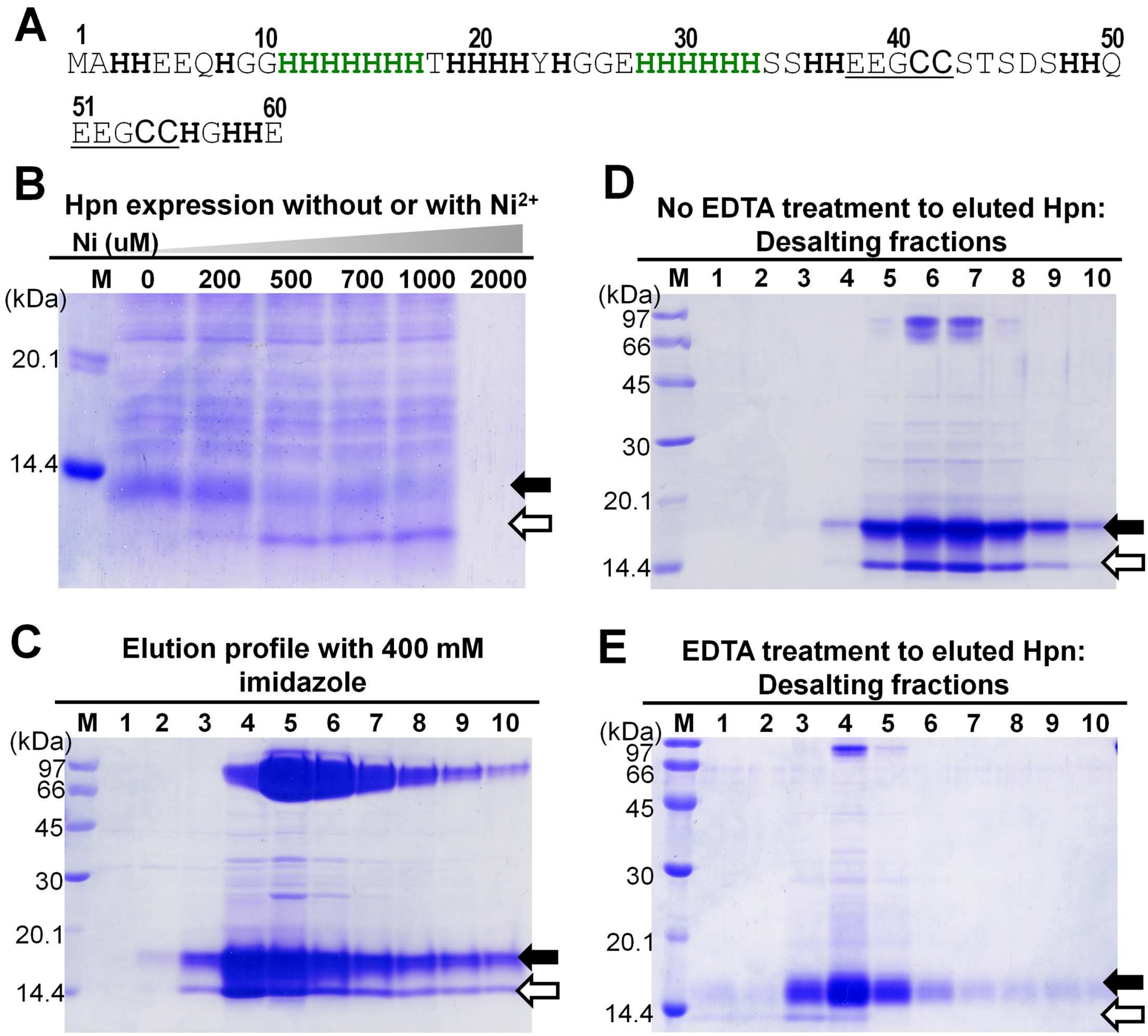

Fig 1. Amino acid sequence, overexpression and purification of recombinant Hpn. Lane M, LMW protein marker standards (GE Healthcare; MW from top to bottom: 97, 66, 45, 30, 20.1 and 14.4 kDa); black arrows depicting apo-Hpn and white arrows showing probable Ni^{2+}-bound Hpn protein in all panels. A. Amino acid sequence of Hpn. Histidine residues are highlighted in bold. Stretches of six and seven histidines are highlighted in green and pentapetide repeats (EEGCC) are underlined. B. SDS-PAGE of Hpn expression with or without Ni^{2+} added in the culture (polyacrylamide-gel 20%). Pellets of 60 μl bacterial cultures were dissolved in 60 μl of 1X Laemmli buffer and boiled for 3 min at 100˚C. Final volume of 15 μl loaded in each lane. C, D and E. Elution profile of purified Hpn checked by loading protein fractions on SDS-PAGE (polyacrylamide-gel 15%). Lanes 1 to 10, fractions of purified protein eluted with 400 mM imidazole (C). Elution profiles of desalted fractions of Hpn without EDTA treatment (D) and with EDTA-treatment (E) were analyzed. Equal volume of 2X Laemmli buffer was added to each eluted fraction and then boiled for 3 min at 100˚C. Total 10 μl applied in each lane in C, D and E.

doi:10.1371/journal.pone.0172182.g001

calmodulin isoforms [32] and Ca^{2+}-dependent protein kinases (CDPKs) [33–36]. Overall, the above observations suggest that there may be an apparent link between metal-binding to Hpn and "gel shifting" pattern. Thus, the anomalous migration of Hpn should be explored in several conditions pertaining to metal binding and its effect on migration rate in SDS-PAGE.

Table 1. List of histidine-rich Ni^{2+}-binding proteins showing gel shifting anomaly.

Protein	Organism	Function	Histidine content	Ni ions per monomer	Formula MW (kDa)	Apparent MW (kDa)	Reference
SlyD	*Escherichia coli*	Ni carrier	10.2%	3	20.8	25	[16,17]
CooC	*Rhodospirillum rubrum*	Nickel accessory protein for maturation of CODH	3%	1	27.8	61, 29	[18]
HypB	*Rhizobium leguminosarum*	GTP-dependent Ni insertase	9.0%	4	32.5	39	[14,15]
HypB	*Archeoglobus fulgidus*	GTP-dependent Ni insertase	2.7%	0.5	24.7	41 (dimer)	[13]
UreE	*Klebsiella aerogenes*	Accessory protein in urease maturation	9.5%	3	17.5	35 (dimer)	[12]
Hpn like	*Helicobacter pylori*	Ni storage	25%	2	9	47, 18	[7]
Hpn	*Helicobacter pylori*	Ni storage	46.7%	5–6	7	>670, 500, 230, 136, 20, 14, 7	Present study and [3]

doi:10.1371/journal.pone.0172182.t001

Also, MW of intact Hpn alongside protein-metal interaction studies by MS could facilitate better understanding of Hpn metallochemistry in detail.

In the present study, an attempt was made to investigate various physicochemical properties of Hpn and not the *in vivo* function of Hpn in *H. pylori* itself. This work was focused on heterologous expression of Hpn in *E. coli*, average molecular mass of purified Hpn, "gel shifting" anomaly with or without Ni^{2+} in different polyacrylamide-gel concentrations and application of MALDI-TOF-MS for studying non-covalent Hpn-Ni^{2+} complexes. To establish a reliable technique to determine MW associated with "gel shifting" anomaly without ambiguity, MW of intact recombinant Hpn was determined by MALDI-TOF-MS using internal protein standards and found to be essentially identical (6945.66±0.34) to the formula MW. Ni^{2+}-treated Hpn migrated more rapidly than untreated Hpn showing differences of 3–4 kDa. This significant metal-triggered shift in electrophoretic gel mobility of Hpn is reported for the first time to the best of our knowledge and termed as a "metal gel-shift". Migration speed of Hpn in both the forms was altered depending on polyacrylamide-gel concentrations. The method for sample and matrix preparation standardized in this study preserved appropriate intermolecular interactions and hence boosts the usefulness of MALDI for the study of non-covalent protein-metal ion complexes.

Materials and methods

Cloning and nucleotide sequencing

All the chemicals and reagents used were of analytical grade or higher. The genome DNA extraction protocol and growth conditions for mouse-adapted strain of *Helicobacter pylori* Sydney strain (*H. pylori* SS1) provided in **supporting information, material and methods section in S1 File**. First, the Hpn encoding region of 1.17 kb was amplified instead of the *hpn* gene only to avoid undesired mutations in the nucleotide sequence of *hpn* `(primers 5'-AGTCCATATGCCTTACACGCCGTAGATGACAAAACGCGC-3' and 5'-GACTGGATCCGGCTCGCTCTCATCTATAGCGTGGCTAAG-3')`. The DNA fragment was cloned into a pBluescript II KS (+) vector (Takara, Japan), and nucleotide sequencing was performed using a BigDye Terminator v3.1 Cycle Sequencing Kit and an ABI PRISM 310 Genetic Analyzer (Applied Biosystems). The *hpn* gene was amplified using the cloned 1.17 kb region as the PCR template `(primers 5'-GACTCATATGGCACACCATGAAGAACAACAC-3' and 5'-GACTGGATCCT`

TATTACTCGTGATGCCCGTGGC-3') and then cloned into pBluscript (Takara, Japan) and pET21b (Novagen, Darmstadt, Germany) vectors. *E. coli* JM 109 and BL21 (DE3) cells purchased from Takara (Japan) were used for the propagation and protein expression with a constitutive (RuBisCo promoter from *Synechococcus* sp. PCC7002) [37]; and isopropyl β-D-1-thiogalactopyranoside (IPTG)-inducible T7 promoter, respectively.

Expression and purification of recombinant Hpn

Recombinant Hpn was purified from harvested cells of 200 ml culture. Harvested cells were suspended in lysis buffer (50 mM Tris-HCl, pH 7.5, and 500 mM NaCl) and purification was done as described previously for His-tagged proteins with some modifications [38]. After sonication (TOMY Ultrasonic Disruptor, duty: 50, output: 4, time: 4 min x 6), supernatant fractions were filtered using Millex®GV filter units of 0.22-μm-pore-size and applied onto a 1-ml HiTrap chelating column (GE Healthcare) that had been equilibrated with start buffer containing 20 mM imidazole, 50 mM Tris-HCl, and 500 mM NaCl. The column was washed with buffer (50 mM Tris, pH 7.5, 50 mM NaCl, and 40 mM imidazole), and then Hpn was eluted using start buffer with 400 mM instead of 20 mM imidazole. Eluted fractions were analyzed for purity using SDS-PAGE (15%), and the purest fractions were applied onto a 5-ml HiTrap desalting column (GE Healthcare) that had been equilibrated with desalting buffer (20 mM Hepes-KOH, pH 7.4, 100 mM NaCl, and 20% glycerol), and purified Hpn was stored at −80˚C until use. The concentration and quality of purified Hpn was measured using bovine serum albumin (BSA) as the standard in a BCA assay (Bio-Rad) in accordance with the manufacturer's instructions and SDS-PAGE (polyacrylamide 15%), respectively.

SDS-PAGE and non-denaturing native-PAGE (native-PAGE)

All purified protein fractions were analyzed by SDS-PAGE in accordance with instructions mentioned previously [39]. A vertical electrophoresis system of mini-slab size from Atto Co. (Japan) was used for the separation of protein samples with appropriate concentrations of polyacrylamide. A LMW-SDS Marker Kit (GE Healthcare) and marker proteins kit from Nacalai Tesque, Inc. (Japan) were used as protein standards in SDS-PAGE. All protein samples were prepared in Laemmli buffer (50 mM Tris-HCl pH 6.8, 10% glycerol, 2% SDS, 7% β-mercaptoethanol and 0.001% bromophenol blue) and then stored at −20˚C before use. The electrophoresis was done till bromophenol blue dye reached to the bottom in all gels of different concentrations (under similar experimental conditions). This optimized method was referred from previous work [27] showing separation of 11 trans-membrane mimetic peptides, translating into MWs of 3.5–41 kDa on 11–18% of polyacrylamide-gel. Resolved proteins were stained with Coomassie Brilliant Blue (CBB) R-250 solution containing 10% acetic acid with 25% methanol.

Fractions of purified Hpn were used for blue native PAGE analysis without boiling or reduction in sample buffer (50 mM Tris with pH 6.8 containing 0.01% bromophenol blue and 10% glycerol). The running buffer was prepared without detergent and consisted of 25 mM Tris, 192 mM glycine, pH 8.0. Stacking gel (4%) and separation gel (10%) were prepared adding suitable buffers, glycerol, ammonium persulfate (APS), and TEMED. Electrophoresis was performed at a constant current of 15 mA and voltage of 160 V and further CBB stained.

Western blotting analysis

The Hpn protein (25 μM) treated with indicated mol equivalent of EDTA or Ni^{2+} resolved on SDS-PAGE (20%) and then electrophoretically blotted onto polyvinylidene fluoride (PVDF) membrane (Amersham Hybond-P, GE Healthcare, code: RPN303F) in transfer buffer containing no methanol. Blotting was performed at 0.8 mA current for every cm^2 area of gel. Proteins were blocked on PVDF membranes in a solution of 5% skim milk for 1 h after washing in PBS-T buffer (phosphate-buffered saline buffer with 0.05% Tween-20, pH 8). The PVDF membrane was further incubated with C-terminal specific-anti 6×histidine monoclonal antibody (9F2) (Wako Japan, product code: 010–21861 diluted to 1:5000 in PBS-T) for 1 h. After three washes of 15:5:5 min in PBS-T, PVDF membrane was then incubated with horseradish peroxidase-conjugated anti-mouse IgG (GE Healthcare, product code: NA931VS, diluted to 1:5000 in PBS-T) for 1 h. The membrane was further washed again with PBS-T as mentioned earlier and Amersham ECL non-radioactive western blotting detection reagents (GE Healthcare) were used for visualizing protein bands in accordance with the manufacturer's instructions.

Hpn interaction with Ni^{2+} ions

For SDS-PAGE and blue native-PAGE analysis, apo-Hpn (25 μM) was prepared as mentioned above and then treated with the indicated amount of Ni^{2+} by adding $NiSO_4$ solution or EDTA (with mol equivalent ratio of 1:6) and incubated for a minimum of 1 h at room temperature. Suitable PAGE buffer was added to the above mixture for loading either on SDS-PAGE (Laemmli buffer) or blue native PAGE (sample buffer used, 50 mM Tris, pH 6.8 with 10% glycerol and 0.01% bromophenol blue). Equal volume of 2X loading buffer was added to protein samples and then applied to native-PAGE directly. For SDS-PAGE, further processing (heat denaturation) done otherwise mentioned in respective figures. Ni^{2+} binding to Hpn protein was investigated using MALDI-TOF-MS by mixing Ni^{2+} or EDTA-treated Hpn with equal amount of matrix solution.

The gel slices of EDTA or Ni^{2+}-treated protein bands resolved on SDS-gel were digested in nitric acid (Nacalai Tesque, Japan) and heated at 80˚C for 10 min, once cooled nitric acid finally diluted to 2%. The Ni^{2+} content was analyzed by ICP-optical emission spectrometry (ICP-OES) (Optima 8300 ICP-OES Spectrometer, PerkinElmer Inc, USA). The standard curve was plotted using a minimum of five standards (ranging from 50 to 1000 ppm) with a blank of 2% nitric acid.

MALDI-TOF-MS

Protein bands resolved on SDS-PAGE were eluted using the protocol described previously [40] with or without CBB staining and then aliquots were used in mass spectrometry. Purified Hpn and elution fractions were directly mixed with an equal volume of matrix solution prepared with different recipes. Acidic and non-acidic matrices were investigated for detecting intact protein-metal ion complexes. Acidic matrix was prepared by mixing 100% acetonitrile (ACN), 0.1% trifluoroacetic acid (TFA), and distilled water (v:v, 50:10:40). Another mild acidic matrix was prepared with the recipe except for more diluted 0.01% TFA. Two different non-acidic matrices were analyzed: 1) sinapinic acid in 100% ACN and distilled water (v:v, 1:1) without TFA [41]; and 2) 4-hydroxy-α-cyanocinnamic acid powder in a saturated solution of ethanol and 1 M ammonium acetate (v:v, 1:1) [42]. MALDI-TOF-MS analysis was done with a Voyager-DE PRO MALDI-TOF-MS (Applied Biosystems). The instrument was calibrated externally with a Sigma Protein MALDI-MS calibration kit. The positive linear mode was set in the instrument to acquire mass spectra using a nitrogen laser (337 nm). An average of a minimum of 150 laser shots was used to accumulate a single spectrum with an accelerating voltage of 25,000 V and extraction delay time of 400 ns. Internal calibration with protein standards (insulin and apomyoglobin), smoothing and baseline correction of the mass spectra was performed and analyzed by using Data Explorer software (Applied Biosystems, MA).

Effect of Ni^{2+} on growth of *E. coli* expressing the *hpn* gene

E. coli cultures, both with pBluscript only and pBluscript-*hpn* plasmid inoculated from individual colonies were grown for overnight in Luria-Bertani (LB) medium containing 100 μg/ml ampicillin at 37˚C. Optical density (OD) of the grown cultures was measured at 600 nm and normalized to 1, of which 100 μl was inoculated to 5 ml of fresh LB medium (1:50 dilution) containing 100 μg/ml ampicillin, and $NiSO_4$ was added where applicable (0, 500, 1000, 1200 μM). Cultures were grown for 4 h at 165 rpm at 37˚C, OD values were measured using U-1800 spectrophotometer (Hitachi, Japan) at 600 nm. Obtained values were normalized against control (culture grown without Ni^{2+} stress) and data from three different replicates was summarized and used to plot the growth curve.

M9 medium is a minimal defined culture medium prepared as described previously [43]. Overnight grown cultures (as above, 100 μl) were inoculated into 5 ml of fresh M9 medium containing 0, 50, and 100 μM $NiSO_4$ and 100 μg/ml ampicillin. These cultures were incubated for 24 h at 165 rpm at 37˚C in a shaker and the growth curve was plotted (as described above).

Ni^{2+} accumulation in *E. coli* expressing the *hpn* gene

Single colonies of transformed *E. coli* JM109 were inoculated into 2 ml of fresh medium (LB or M9) supplemented with appropriate concentrations of Ni^{2+}. Overnight grown cultures (after normalizing OD to 1) were inoculated into 5 ml of fresh medium and grown for 24 h at 37˚C with and without Ni^{2+}. Sampling (2 ml culture) was done at 24 h (LB and M9), respectively. Cells were centrifuged at 15000 rpm for 1 min and bacterial pellet was washed with GET buffer (50 mM glucose, 25 mM Tris-HCl, 10 mM EDTA) followed by drying at 80˚C for a minimum of 3 h. The dried pellet was digested in nitric acid (Nacalai Tesque, Japan) and heated at 80˚C for 10 min, once cooled nitric acid finally diluted to 2%. The Ni^{2+} content incorporated inside the cell and total uptake were analyzed by ICP-OES.

Results

Overexpression and purification of Hpn

Four changes were observed at the nucleotide level in the *hpn* ORF of strain SS1 compared with strain 26695, but it had no change at the amino-acid level (**Supporting information, Fig A in S1 File**). Hpn expression in *E. coli* culture was standardized in LB medium. The molecular mass of Hpn expressed with and without Ni^{2+} was investigated by SDS-PAGE with a crude cell extract and found to be different (**Fig 1B**). It has been shown that Hpn forms a range of multimeric complexes estimated by chromatographic techniques. The number and size of multimers was changed depending on the buffer composition and treatment of DTT, imidazole or Ni^{2+} [3]. However, SDS-PAGE pattern of multimeric solution was not investigated. An attempt was made to explore the differential migration when expressed with or without Ni^{2+} and SDS-PAGE pattern of recombinant Hpn obtained at different steps of chromatographic purification.

The SDS-PAGE pattern of imidazole-eluted Hpn showed three major protein bands of approximately 14 kDa, 18 kDa, and 70 kDa on 15% polyacrylamide-gel (**Fig 1C**). The SDS-resistant oligomeric complex (~70 kDa) was highly stable and unaffected by reducing agents such as β-mercaptoethanol or boiling (100˚C for 3 min). After desalting, this ~70 kDa band was observed but at very low concentration, thereby suggesting the role of imidazole in interconversion of Hpn multimeric forms (**Fig 1D**). The other two protein bands of ~14 kDa and ~18 kDa were observed corresponding to the pattern of the crude extract with and without Ni^{2+} respectively. This indicates that a trace of Ni^{2+} was present in purified Hpn incorporated during the purification process. Thus, the purified Hpn was used after removing trace amounts of Ni^{2+} by treating with EDTA during buffer exchange with desalting columns (**Fig 1E**).

It has been shown that Hpn forms a range of multimeric complexes depending on buffer composition and treatment of DTT, imidazole and Ni^{2+} estimated by gel-filtration chromatography [3]. Consistent with earlier report, Hpn protein (25 μM) treated with either EDTA or Ni^{2+} (mol equivalent ratio of 1:6 independently) migrated as a range of multimeric species on 10% native-PAGE gel (**Supporting information, Fig B in S1 File**).

Confirmation of recombinant Hpn by western blotting

The post-translational removal of N-terminal methionine (149.21 Da) in wild-type (in *Helicobacter pylori*) and recombinant Hpn (in *E. coli*) is reported [2,3]. Therefore, the monoisotopic and average molecular mass (abbreviated as M_{MONO} and M_{av}) of Hpn without N-terminal methionine were estimated using PAWS software (http://www.proteometrics.com) as 6941.288 Da and 6946.01 Da, respectively. Hpn appeared to migrate faster in the sample from cells cultured with Ni^{2+} compared to that without Ni^{2+} on 15% (**Fig 1C–1E**) or 20% SDS-PAGE (**Fig 1B**), but neither of the conditions showed the migratory position for an expected MW i.e. ~7 kDa.

To facilitate the identification of Hpn protein (untagged) precisely, western blotting was performed using a His.Tag® monoclonal antibody assuming that the His.Tag® antibody would bind to Hpn at the seven and six residue histidine repeats [3]. Recombinant Hpn (untagged) confirmed a thin band in western blot (**Fig 2A**, left panel) corresponding to the migration position of apo-Hpn but Ni^{2+}-treated Hpn was barely visible. CBB staining of same PVDF membrane showed both the protein bands but small amount of Ni^{2+}-treated Hpn remain bound to membrane (**Fig 2A,** right panel). Possible explanation is that untagged Hpn, specifically metalated form may have weaker binding affinity to membrane probably due to its atypical chemical nature. Furthermore, we investigated effect of metal binding to Hpn when fused with another protein (GFP-Hpn and GFP- His_6). This was done to know the effect of differential co-ordination geometry of metal-binding and its chemical surrounding on Hpn-antibody interaction (**Supporting information, result section; Fig C in S1 File**). The relative detection sensitivity of Ni^{2+}-treated protein with His.Tag® antibody in enzyme-linked immunosorbent assay (ELISA) give order of untagged Hpn $<$ GFP-Hpn $<$ GFP-His_6. Hence, the variability that we observed in detection of apo- and metalated-Hpn on western blots may have resulted not only from membrane-binding efficiency but also from differential exposure of His-rich region upon metal-binding.

Determination of MW by MALDI-TOF-MS

To quantify the reliable molecular mass of untagged Hpn, MALDI-TOF-MS was used for purified apo-Hpn with an acidic matrix in linear positive mode. As shown in **Fig 2B**, integral signals of four heteromeric species of Hpn (M^+, $2M^+$, $3M^+$, and $4M^+$) were observed with a major peak of singly charged Hpn[M^+]. Although a tendency of apo-Hpn to form multimeric complexes in native and reduced states was confirmed by native-PAGE and SDS-PAGE (with 400 mM imidazole-buffer), respectively, the appearance of a major peak of monomer and low intensity peaks of heteromeric species in MALDI-TOF-MS analysis is of a great advantage in determining the molecular mass accurately.

Insulin (M_{MONO} 5729.6009; M_{av} 5734.51) and apomyoglobin (M_{MONO} 16940.9650; M_{av} 16951.49) were used as internal standards for mass calibration while acquiring spectra. The M_{av} of Hpn was determined as 6945.66±0.34 Da calculated from the average of at least five different measurements. A representative calibrated peak of Hpn[M^+] with *m/z* 6946.05 is shown

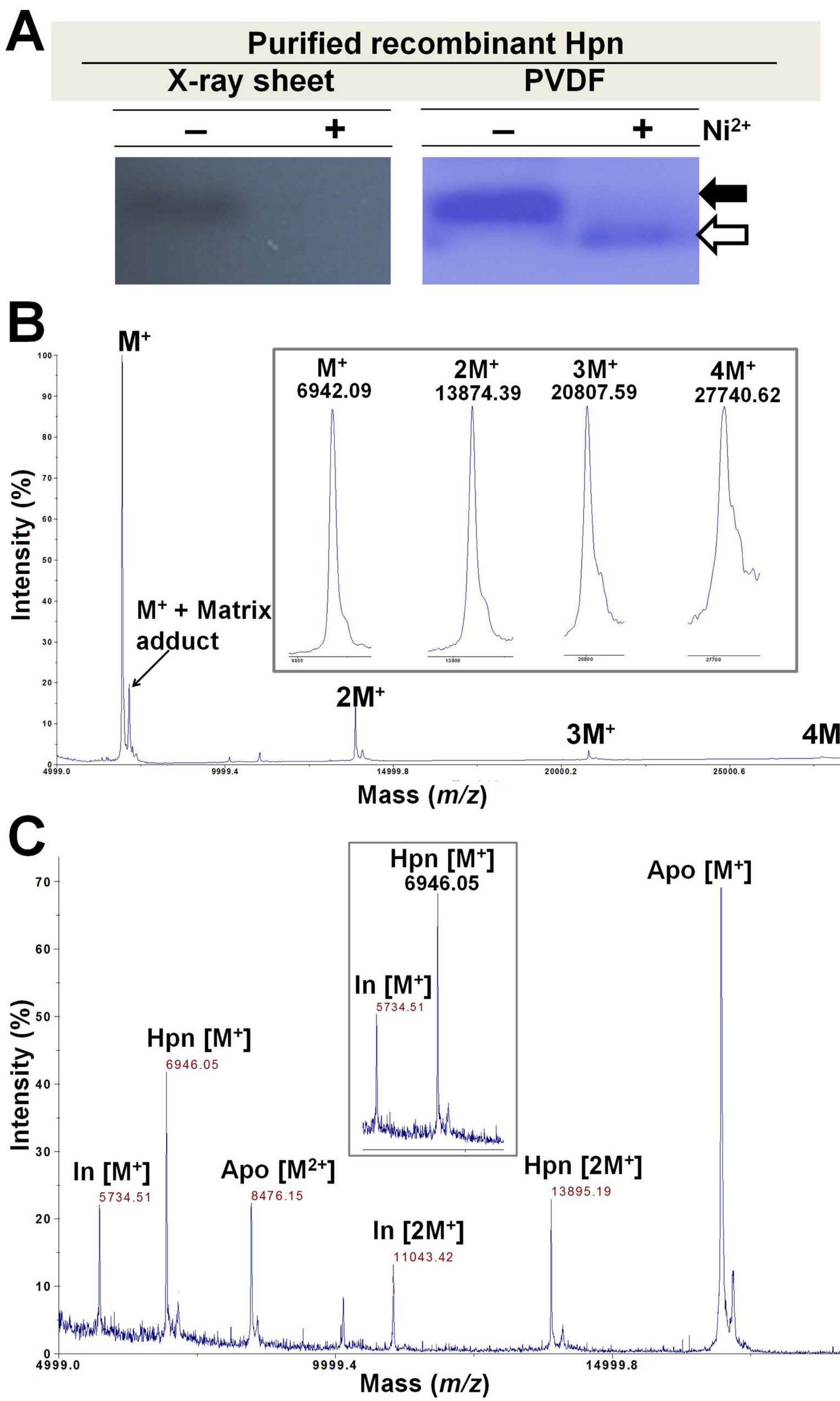

Fig 2. Western blot and molecular mass analysis of Hpn with MALDI-TOF-MS. A. Western blot of Hpn was done using His.Tag® monoclonal antibody. In left panel, X-ray sheet showing ECL detection result of

recombinant Hpn (with and without Ni^{2+}) and right panel showing same CBB-stained-PVDF membrane used for ECL detection. B. Sharp peak of monomeric Hpn together with neighboring small peak of matrix adduct, and three oligomeric species with lower intensity was observed in Hpn spectrum. The monomeric and three oligomeric species: M^+, $2M^+$, $3M^+$, and $4M^+$ with masses of *m/z* 6942.09, 13874.39, 20807.59, 27740.62 respectively are shown in inset. C. Molecular mass of Hpn was measured (*m/z* 6946.05) using two different internal standards (insulin and apomyoglobin), which showed peaks for protonated and doubly charged species. Average MW of recombinant Hpn (without methionine) determined (6945.66±0.34) is showing almost negligible difference (0.35) compared to theoretical MW (6946.01).

doi:10.1371/journal.pone.0172182.g002

in Fig 2C. However, MALDI-TOF-MS analysis confirmed that the M_{av} of purified recombinant Hpn was 6945.66±0.34 Da instead of the calculated molecular mass of 7,077 Da. This suggests the loss of the N-terminal methionine residue (*m/z* 149.21), probably in post-translation process in *E. coli* and this observation is consistent with the previous reports [2,3].

Hpn exhibits both "gel shifting" and "metal gel-shift"

The reduction by β-mercaptoethanol and boiling before gel loading of purified Hpn had no effect on the appearance of two bands even in different polyacrylamide-gel concentrations [(~14 kDa and ~18 kDa on 15% SDS-PAGE; Fig 1C–1E) and (~7 kDa and <7 kDa on 20% SDS-PAGE; Fig 3A)]. This was further analyzed by Ni^{2+} addition and removal (using EDTA) separately to the purified Hpn. In both cases, samples with and without boiling were analyzed in order to assess if Hpn showed a characteristic property of "heat modifiability" like outer membrane proteins (OMPs) from *E. coli* [44]. The concept of heat modifiability constitutes preservation of both folded and unfolded structures upon SDS treatment to purified OMPs but with no heat and shows two different bands on SDS-PAGE. Heating denatures the folded β-content of OMPs and SDS-PAGE data shows single band. No difference in migration pattern was observed between heated and non-heated samples of Hpn indicating the absence of heat modifiability (Fig 3A).

Moreover, EDTA-treated Hpn showed only one band of ~7 kDa on 20% polyacrylamide-gel. On the other hand, the only protein band observed in Ni^{2+}-treated Hpn was of compact lower-size <7 kDa. Appearance of only one of the either band demonstrates that both bands were derived from same protein i.e. Hpn. The partially-metalated Hpn treated with relatively lower mol equivalent proportion of Ni^{2+} (0.0, 0.8, 1.2, 1.6, 2.0, 2.4, 2.8, 3.2, 3.6, 4.0, 6.0 and 8.0) demonstrated gradual shift with decrease in homogeneity of upper band followed by increased intensity of compact lower band (Fig 3B).

The Hpn protein treated for SDS-PAGE analyses was directly used for MALDI-TOF-MS measurements and mass spectra of Ni^{2+}-treated Hpn only showed peaks for protein-metal complexes (Fig 3C). The mass spectra of protein fractions eluted from SDS-gel corresponding to ~7 kDa and compact <7 kDa on 20% gel were measured. Only lower compact band (<7 kDa) confirmed mass spectra for partially preserved protein-metal complexes (Fig 3C). This MS data prompted us to quantify the metal-content of SDS-gel-eluted bands. The Ni^{2+} content in lower compact bands (combining several gel slices together) was detectable in ICP-OES. Measurements for EDTA-treated Hpn band were below the detection limit signifying no metal bound to Hpn protein.

Several studies have reported preservation of protein-metal complex in SDS-PAGE and also in MALDI technique **(supporting information, Table B and C in S1 File)**. Thus, those studies have provided experimental evidence that some metal-binding proteins/metalloproteins can retain protein-metal complex even after using "harsh" experimental protocols (i.e. use of SDS, denaturing agents, acidic matrices, organic solvents or heating). Therefore, it is postulated that the methodology employed in the present study was able to detect Hpn-Ni^{2+}

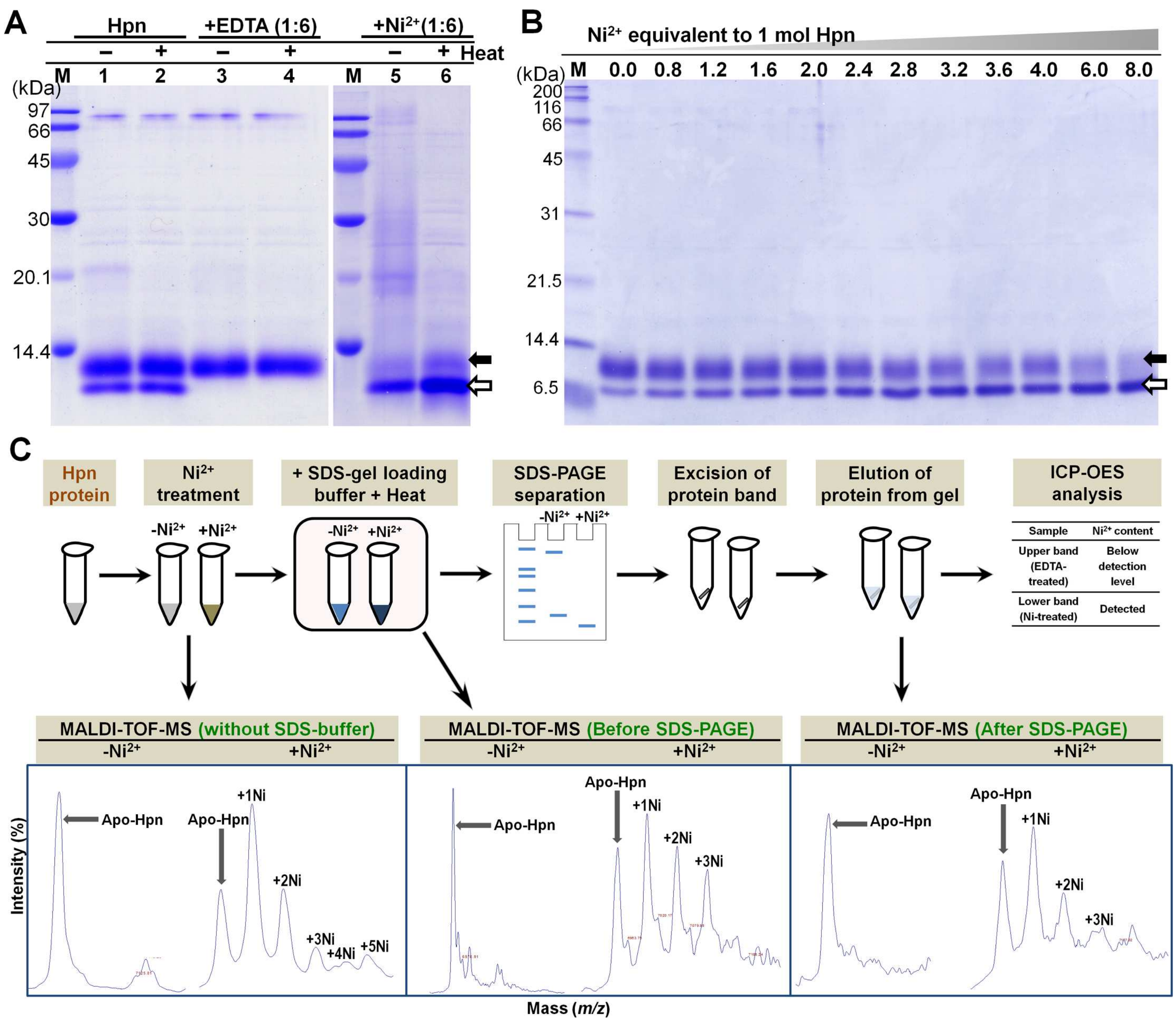

Fig 3. Confirmation of "Metal gel-shift" mechanism. A. Effect of EDTA and Ni^{2+} ion treatment on migration rate of recombinant Hpn in SDS-PAGE (polyacrylamide-gel 20%). Lane M, protein marker (GE Healthcare; MW from top to bottom: 97, 66, 45, 30, 20.1 and 14.4 kDa); lane 1 and 2, Hpn before and after boiling (3 min at 100˚C), respectively; lanes 3 and 4, EDTA-treated Hpn without and with boiling, respectively; lanes 5 and 6, Ni^{2+}-treated Hpn without and with boiling, respectively. B. The SDS-PAGE analysis of partially-metalated-Hpn (25 μM) treated with increasing concentration of Ni^{2+} (1:0, 1:0.8, 1:1.2, 1:1.6, 1:2.0, 1:2.4, 1:2.8, 1:3.2, 1:3.6, 1:4.0, 1:6.0 and 1:8.0). Lane M is marker proteins standard from Nacalai Tesque (200, 116, 66, 45, 31, 21.5, 14.4, 6.5 kDa from top to bottom respectively). Equal volume of heat-denatured protein applied in each lane. C. Scheme used for MALDI-TOF-MS analysis of Hpn protein that was heat denatured in Laemmli buffer. MS data was measured for Hpn treated with or without Ni^{2+} ion (1:6 mol equivalent ratios). Further, MS data for Hpn (with or without Ni^{2+}) treated in Laemmli buffer (before and after SDS-PAGE) was measured. Even though some interference due to adducts was observed in samples treated with Laemmli buffer or gel-eluted fractions, metalated peaks (showing Hpn-Ni^{2+} complexes) were distinct. The occurrence of metalated peaks was observed only for Ni^{2+}-treated Hpn in all the conditions.

doi:10.1371/journal.pone.0172182.g003

complex and it was not a consequence of artifact formation. Previous circular dichroism (CD) studies have reported more compact structure (an increase in β-sheet with reduced α-helical content) after Ni^{2+} binding to Hpn [3,4].

Taken together, these data indicate that preserved protein-metal complex forms a more compact structure leading to faster migration on SDS-PAGE. This phenomenon of reversible shift in position when treated with either EDTA or Ni^{2+} was termed as "metal gel-shift".

Polyacrylamide-gel concentration determines migration rate of Hpn on SDS-PAGE regardless of "metal gel-shift"

Polyacrylamide-gel concentration can dictate the migration speed of some polypeptides [27]. To test the hypothesis that "metal gel-shift" is related to only Ni^{2+} binding to Hpn or whether gel percentage has an effect on it, we thoroughly analyzed gel mobility of apo-Hpn and Ni^{2+}-treated Hpn with different polyacrylamide-gel concentrations. This concept was investigated with purified Hpn after removing trace amounts of Ni^{2+} (Fig 4A). The migration distance of apo-Hpn and Ni^{2+}-treated Hpn relative to marker proteins (Nacalai Tesque, Inc. Japan) was analyzed using ImageJ software [45] (**protocol provided in Supporting information, Annexure A in S1 File**). Outcomes from these experiments were in agreement with our hypothesis; the Ni^{2+}-treated Hpn migrated faster than untreated Hpn showing MW difference of 3–4 kDa (Fig 4B). These results demonstrated that apo-Hpn migrated slowly in contrast to Ni^{2+}-treated Hpn in all analyzed polyacrylamide-gel concentrations, signifying that "metal gel-shift" is intimately associated with Ni^{2+}-binding to Hpn. This also shows that higher polyacrylamide-gel concentrations resulted in faster migration of both the forms on SDS-PAGE (with and without Ni^{2+}).

Analysis of non-covalent Hpn-Ni^{2+} complexes

We evaluated inter-conversion of Hpn-metal complexes using purified Hpn by MALDI--TOF-MS. Although non-covalent complexes are expected to be stable at physiological pH, acidic conditions or organic solvents used in matrix preparation may not be the only factors important in the dissociation and prevent detection of these complexes in MALDI analysis [46]. In this work, we applied full-length Hpn protein for studying Ni^{2+} binding. First, we standardized the set of conditions for acquisition of spectra for intact Hpn, and then we investigated different types of matrices to analyze protein-metal ion complexes. Among the tested combinations of acidic and non-acidic matrices, we found a mildly acidic matrix (100% ACN, 0.01% TFA, and distilled water; v:v, 50:10:40) was most suitable in our experimental conditions, and this was used in subsequent spectral measurements. This is the first study reporting the successful application of MALDI-TOF-MS for investigating protein-Ni^{2+} ion complexes. The MS data showed the progressive appearance of all possible metal-bound species of Hpn, signifying that binding of metal ions at each site on protein may occur independently. Moreover, a decrease in spectral intensity of the apo-protein with increasing amounts of Ni^{2+} and increased intensity of metalated species provided conclusive evidence for the binding of Ni^{2+} to Hpn.

To evaluate Ni^{2+} binding, Hpn treated with increasing molar concentrations of $NiSO_4$ solution was analyzed. Generally, the peaks of protein-metal complexes are smaller than the peak of the apo-protein, even if a protein-metal interaction is already known to exist. Therefore, higher amounts of Ni^{2+} were added to Hpn after confirming that no obstruction was caused by it in the MALDI spectrum. Ni^{2+} solution was added to apo-Hpn (25 μM), pH 7.5 at an increasing mol equivalent ratio of Hpn to Ni^{2+} ion. After 1 h incubation at room temperature, protein-metal solution was mixed with matrix and MS were acquired as described above (Fig 5).

Representative MS of metalated species of Hpn clearly detected a progression with seven major peaks (at *m/z* 6937.66, 6993.06, 7049.55, 7105.76, 7162.59, 7218.94, and 7275.33). The MS showed peaks of diverse intensity ranging from two to six Ni^{2+} ions bound to Hpn (Fig 5A), A

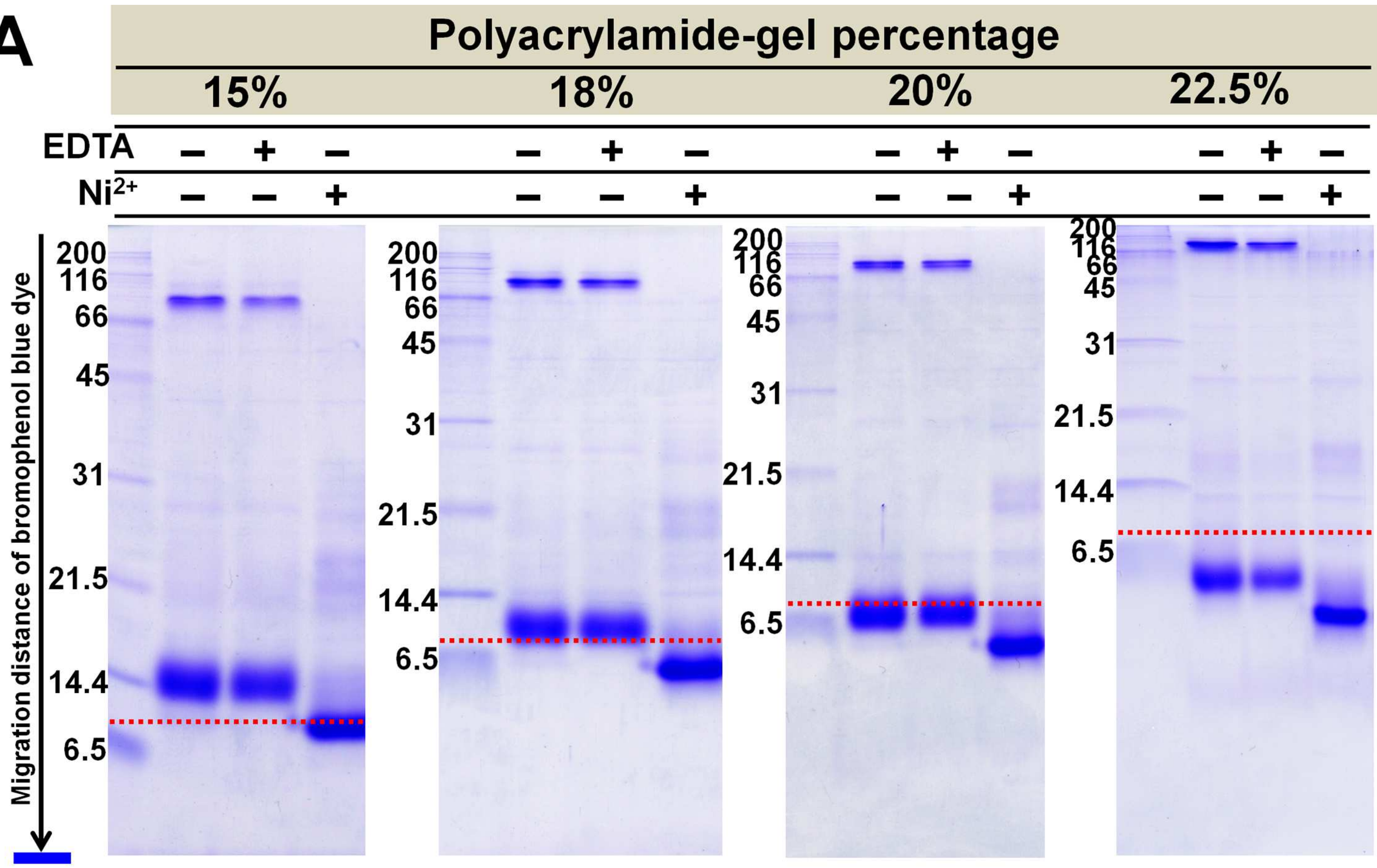

B

Polyacrylamide-gel	15 %	18 %	20 %	22.5 %
Apo-Hpn (kDa)	14.7	11.7	9.7	4.9
Ni^{2+}-Hpn (kDa)	11.3	8.2	6.4	0.8
Difference between Apo-Hpn and Ni^{2+}-Hpn (kDa)	3.4	3.5	3.3	4.1

Fig 4. Effect of polyacrylamide-gel concentration on migration speed of recombinant Hpn without or with metal-treatment on SDS-PAGE. A. Relative position of apo- and Ni^{2+}-treated Hpn protein depending on the polyacrylamide percentage (15, 18, 20 and 22.5%) in gels. Lane M is marker proteins standard from Nacalai Tesque (200, 116, 66, 45, 31, 21.5, 14.4, 6.5 kDa from top to bottom respectively). The SDS-gel electrophoresis was done till bromophenol blue dye reached to the bottom in all gels. Therefore, theoretical MW values for marker proteins- lysozyme (14.4 kDa) and Trypsin inhibitor (21.5 kDa) were taken into consideration for estimation of apparent MW using ImageJ software (**protocol provided in Supplementary information as Annexure A**). Red dotted line depicts expected position corresponding to theoretical MW (~6.9 kDa). B. The apparent MW of apo- and Ni^{2+}-treated Hpn separated on different polyacrylamide-gel concentrations was estimated by comparing relative migration distance of Hpn with globular marker proteins on SDS-PAGE.

doi:10.1371/journal.pone.0172182.g004

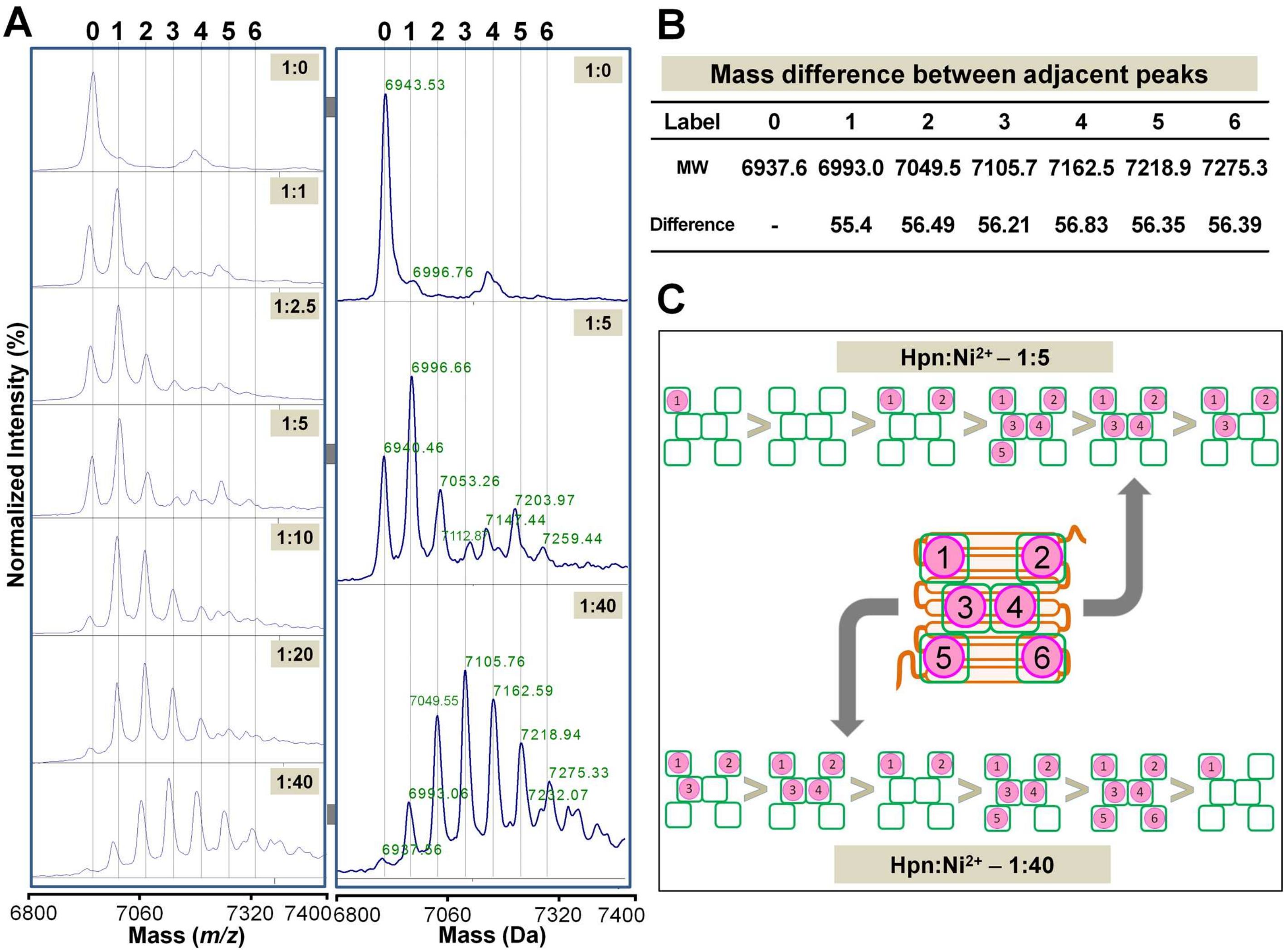

Fig 5. MALDI-TOF-MS analysis of Ni^{2+} binding to Hpn. A. Spectra obtained with increasing concentrations of Ni^{2+} (1:0, 1:1, 1:2.5, 1:5, 1:10, 1:20 and 1:40, mol equivalent from top to bottom, respectively) added to apo-Hpn (25 μM) shown in the right panel, and enlarged view of three representative spectra (1:0, 1:10 and 1:40) shown with molecular mass of each peak in the left side. Numbers above dotted line correspond to the number of Ni^{2+} bound to Hpn protein. B. Mass difference calculated between adjacent peaks was found to be approximately equal to the molecular mass of the Ni^{2+} ion (58.69) with the loss of two H^+ atoms (molecular weight [MW] of H^+ = 1.00794) upon metal binding. C. Model of Ni^{2+} ion binding to Hpn. Order of occurrence has drawn on the basis of peak intensity obtained in MALDI-TOF-MS data.

doi:10.1371/journal.pone.0172182.g005

with no specific species dominant in all the measured protein to metal ratios. The mass differences between adjacent peaks were about *m/z* 56.7 (Fig 5B), matching the added Ni^{2+} ion (*m/z* 58.69 of Ni^{2+}) with the loss of two hydrogen residues during the ionization (*m/z* 1.007825×2). Overlay analysis of MS with and without Ni^{2+} showed slight mass differences (*m/z*) between expected and observed molecular masses may be due to tightly bound ions as previously observed for UreE protein from *H. pylori* [47]. The seventh and subsequent peaks were bifurcated possibly because of matrix adducts interference and hence considered not reliable for assignment to Hpn-Ni^{2+} ion complex. Titration of Hpn with relatively lower Ni^{2+} concentrations (1:5) indicated at least one preferential higher-affinity site, peak intensities of the protein-metal complexes were not according to the loading number of Ni^{2+} ions on binding sites of Hpn (1>0>2 >5>4>3). Furthermore, a difference in peak intensity with higher amounts of Ni^{2+} (1:40) was observed (3>4>2>5>6>1) suggesting the presence of several binding sites with different affinity. The progressive appearance of peaks for all of the possible Hpn-Ni^{2+} ion complexes implied that Ni^{2+} binding to Hpn occurred in a non-cooperative way (Fig 5C) as reported in cysteine-rich human metallothionein 1a [48] and histidine-rich *E. coli* SlyD protein [17].

Ni^{2+} tolerance and accumulation in Hpn-expressing *E. coli* cells

If there is higher metal accumulation inside cells expressing the recombinant metal-binding protein, then it should show better cell growth with higher tolerance compare with wild-type upon addition of higher amounts of metal to the culture. However, this phenomenon was not observed in the current as well as previous studies in Hpn-producing *E. coli* cells (Hpn+) compared with wild-type (Hpn–) grown in LB medium [3]. Even though Hpn have more efficient metal-binding ability as observed in MALDI-TOF-MS analysis, higher Ni^{2+} accumulation measured by ICP-OES (6× for Hpn+ compared with Hpn–) was not correlated with higher tolerance and cell survival (<twice in Hpn+ compared with Hpn–) (**Fig 6A–6C**). We hypothesized that an unknown composition of nutrients in LB medium may compensate for toxicity or availability of free Ni^{2+} ion to cells. Therefore, we tested M9 medium with a defined nutrient composition. As shown in **Fig 6D and 6E**, there was almost no further growth of wild-type (Hpn–) at 50 μM and 100 μM Ni^{2+} supplied in M9 medium but Hpn producing cells (Hpn+) were grown normally with approximately 30 and 45 times higher intracellular Ni^{2+} content respectively (**Fig 6F**).

Discussion and conclusions

The main findings of current work are as follows: 1) Hpn forms multimers in native state as well as SDS-resistant multimer when eluted with 400 mM imidazole in buffer; 2) Ni^{2+}-binding to Hpn altered antibody binding in western blot and ELISA signifying differential exposure of His-rich region upon metal-binding; 3) higher polyacrylamide-gel concentrations resulted in faster migration of Hpn in SDS-PAGE; 4) average molecular mass of Hpn determined as *m/z* 6945.66±0.34; 5) Hpn forms SDS-resistant (preserved) protein-metal complexes and exhibits metal-triggered shift in electrophoretic mobility causing "metal gel-shift" mechanism; 6) MALDI-TOF-MS was effectively employed to study non-covalent Hpn-Ni^{2+} ion complexes showing up to six Ni^{2+} ions bound per monomer in a non-cooperative way suggesting an equilibrium between Hpn-metalated species dependent on metal availability. These findings explore various unusual physicochemical aspects of Hpn. Also, higher tolerance and Ni^{2+} accumulation in Hpn-expressing *Escherichia coli* than wild-type in minimal (M9) and nutrient-rich (LB) supply suggests protective role and potential to load higher amounts of Ni^{2+} that corroborating with MALDI-TOF-MS data.

The Hpn protein contains remarkably high number of histidine residues, mostly in clusters (**Fig 1A**). Histidine is unique in its molecular structure with an imidazole ring in its side chain (an aromatic motif), and this can act as a ligand for metallic cations and as a hydrogen bond donor or acceptor. "Stacking" behavior of the aromatic rings of histidine can be one possible mechanism responsible for the formation of non-covalent multimeric complexes; however, this concept is yet to be understood clearly in multimeric proteins [49]. Elution buffer containing imidazole (400 μM) led to formation of SDS-resistant multimer that survived even in reduction and heat denaturation but converted to apparent monomer in denatured Ni^{2+}-treated Hpn (**Fig 4**). The preserved SDS-resistant protein-protein oligomer is reported for several proteins under certain chemical environment (**Supporting information, Table A in S1 File**) [50–55].

Gel shifting

Protein migration can be affected by several factors including molecular size, shape, net charge, MW of the protein, and polyacrylamide concentration [27]. SDS normally binds at

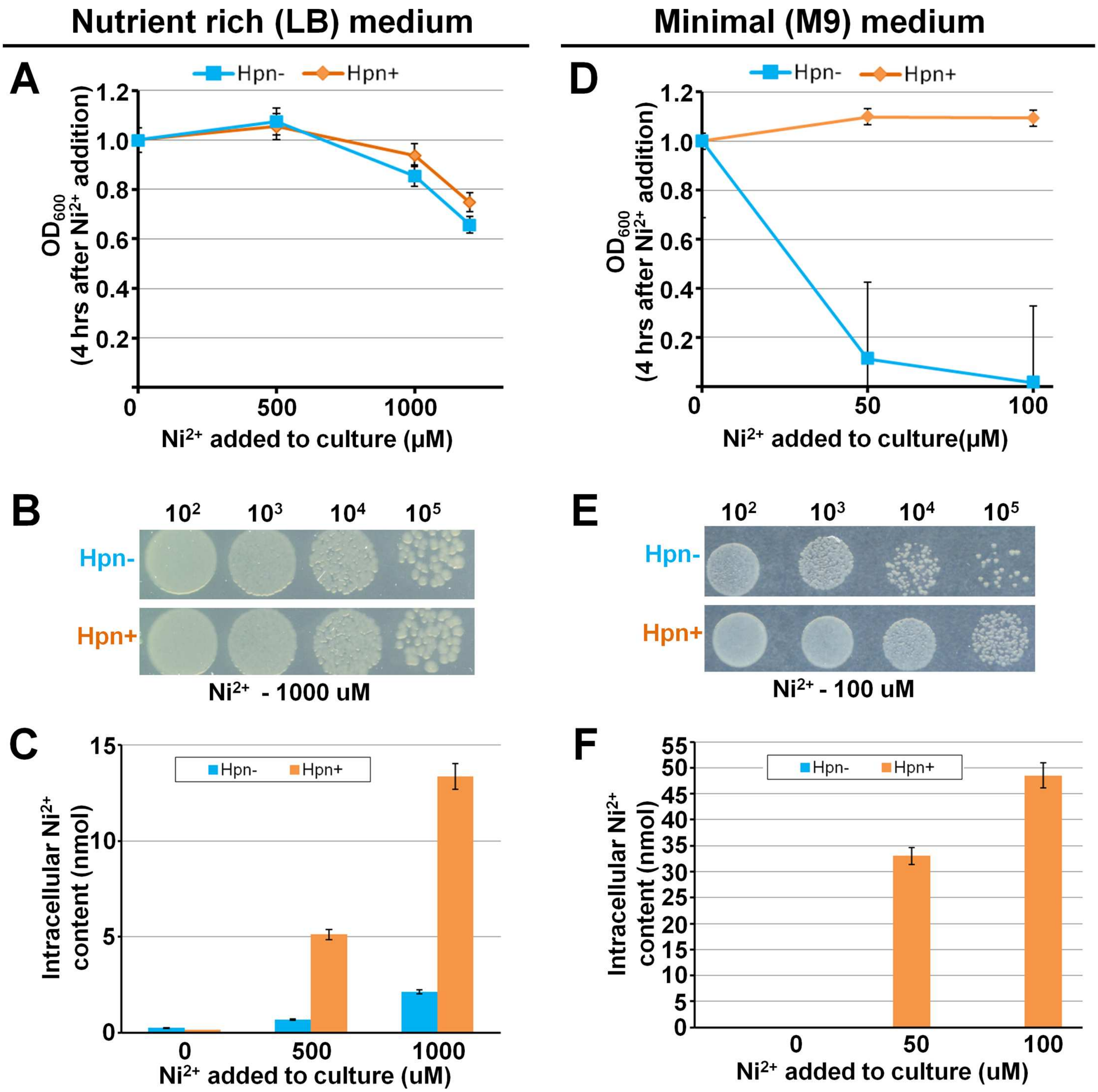

Fig 6. Ni^{2+} tolerance, cell survival, and accumulation in Hpn-expressing *E. coli*. Effect of Ni^{2+} on growth of *E. coli* in Luria-Bertani (LB) (panel A) and M9 medium (panel D). Growth curve was plotted in terms of optical density (OD) against amount of Ni^{2+}added to culture. Cell survival under Ni^{2+} stress analyzed by dots blot as shown in panel B (LB) and E (M9). Panel C (LB) and F (M9) represent the intracellular Ni^{2+} content in *E. coli* expressing *hpn* gene compare to that of without *hpn* gene.

doi:10.1371/journal.pone.0172182.g006

hydrophobic sites, therefore it is reasonable that denatured apo-Hpn migrates at a slower rate compared with marker proteins, because of the higher amount of hydrophilic residues and only one hydrophobic amino acid in the Hpn [19,21,24]. A smaller protein with a higher number of hydrophilic residues may have a greater hydrodynamic radius than a larger protein but weaker hydration [56]. Similar results are reported for cystic fibrosis transmembrane conductance regulator for the reason that of a change in helical structure altered SDS-binding indicating protein-SDS complex size was a more important factor than net charge [19] and its interaction with the sieving effects of a polyacrylamide gel [21].

The SDS-PAGE data demonstrated that the polyacrylamide-gel concentration affects the migration rate of Hpn. Similar results are observed in "gel shifting" patterns for transmembrane proteins in SDS-PAGE [27]. This indicate as any factor that changes effective molecular size and net charge of protein-SDS complex can affect migration speed depending on polyacrylamide-gel concentration, specifically affecting its interaction with the available space in SDS-gel matrix [19,20,27]. In case of Hpn, impact of "stacking" behavior seems to exceed all other factors and may control the migration speed depending on polyacrylamide-gel concentration. Taken together, interplay between protein-protein interaction and sieving effects of gel matrix may be a significant factor that influences gel mobility.

Metal gel-shift

Generally, non-covalent interactions should disrupt during SDS-PAGE owing to activity of SDS and reducing agent [53]. However, preservation of protein-metal complex in SDS-PAGE is reported in several cases, possibly due to incomplete or "reconstructive denaturation" (**Supporting information, Table B in S1 File**) [31,32,53,55,57–62]. Preservation of partial Hpn-Ni^{2+} complex even after electrophoretic separation implies significant strength and stability of Hpn-Ni^{2+} bond. Although exact mechanism of resistance to reduction or denaturation and retaining metal ion is not yet known, similar results were observed in case of platinum-binding proteins [63].

The change in electrophoretic mobility on SDS-PAGE after metal-binding to a protein is rarely acknowledged except for some Ca^{2+}-binding proteins including calmodulin isoforms [32,33]. The wild-type and recombinant CDPKs from soybean [34], tobacco [35] and Arabidopsis [36] display shift in electrophoretic mobility on SDS-PAGE and migrate faster or slower depending on Ca^{2+} availability and is probably due to Ca^{2+}-induced conformational change [36]. The protein band of apo-Hpn was not as sharp as that of Ni^{2+}-treated Hpn, which might be caused by conformational changes upon metal binding. Thus, higher degree of compactness or somehow altered SDS-binding to protein-metal complex that may allow faster migration of Ni^{2+}-treated Hpn than apo-Hpn. Faster migration on SDS-PAGE of unreduced against reduced lysozyme [64] and for a membrane protein OmpA [65] also suggested a possible role of structural compactness in "gel shifting". Considering added MW of metal ions, theoretical MW of Hpn protein in "metal-gel shift" band is higher than apo-Hpn band. On the contrary, "metal-gel shift" band is migrating faster to lower position compared to apo-Hpn band indicating conformational change (and not actual MW) is decisive in governing migration rate.

From the experimental results, mechanism of "gel shifting" and "metal gel-shift" can be described as shown in **Fig 7**. Anomalous migration of apo-Hpn (scheme highlighted with yellow background) or metal-bound Hpn (scheme highlighted with green background) might be due to differential amounts of SDS bound to protein, histidine stacking, altered hydrodynamic radius, degree of compactness after metal-binding, or a combination of either of these factors. The different structures are illustrated and discussed thoroughly in **Fig 7**. Nevertheless, there might be additional biochemical and biophysical processes governing differential protein migration in SDS-PAGE that is not explained in this scheme.

The binding of non-denatured Hpn to Ni^{2+} column and reversible "metal-gel shift" in SDS-PAGE presented herein together with previous CD studies [3] indicated that Hpn protein

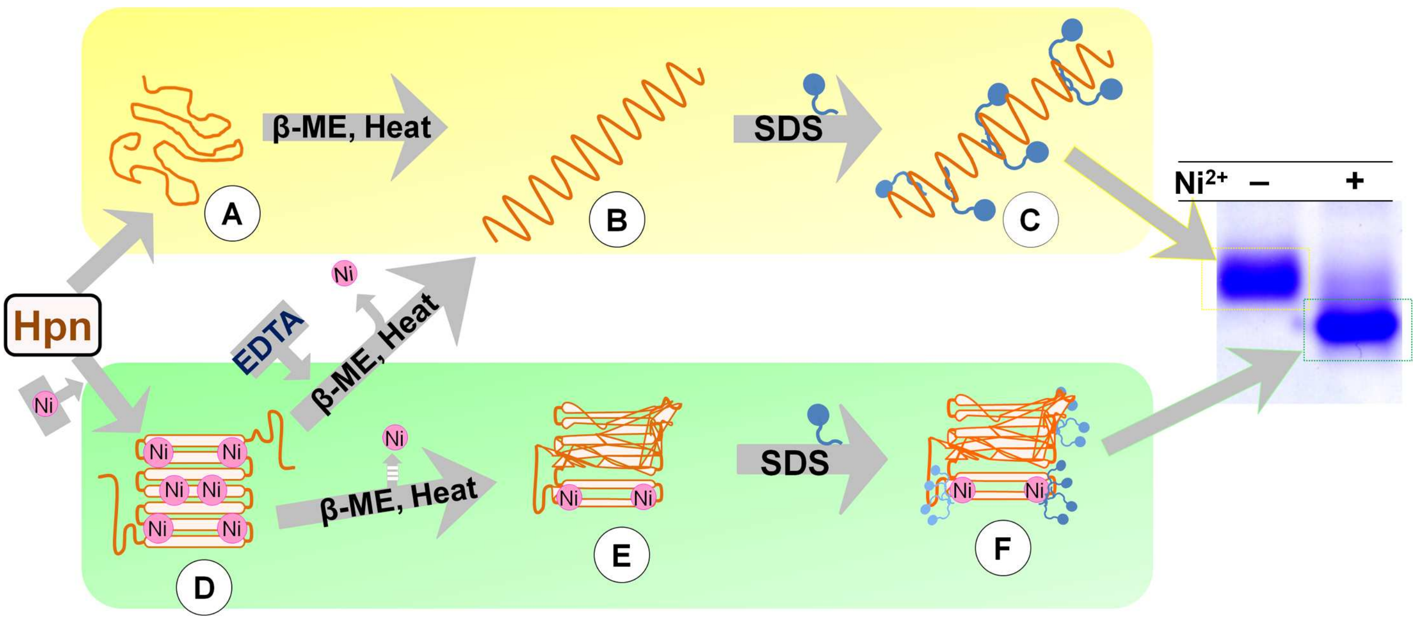

Fig 7. Probable interrelationship between differential electrophoretic mobility of Hpn and Ni^{2+} binding. Hpn may not have a definite form in the absence of Ni^{2+} (A). After denaturation (B), smaller amounts of SDS binding/stacking behavior/larger hydrodynamic radius as well as a combination of some or all of these conditions (C) might have resulted in slower migration on SDS-PAGE (scheme highlighted with yellow background). Ni^{2+}-treated Hpn forms a more compact structure (D). Pictorial structure of metalated Hpn is drawn to explain the model. MALDI spectra showed a partial Ni^{2+} bound form (E) in denatured SDS-PAGE. Altered binding of SDS (F) caused by replacement of protein-protein to protein-SDS contacts (inhibiting stacking behavior) and/or degree of compactness (or reduced hydrodynamic radius) may be key factors responsible for "metal gel-shift" (scheme highlighted with green background). β-ME, β-mercaptoethanol; EDTA, ethylene diaminetetraacetic acid.

doi:10.1371/journal.pone.0172182.g007

could easily exchange metal ion suggesting the position of metal-binding domains are solvent exposed and present at Hpn surface. Metal-induced structural changes leading to the formation of a definite form has been reported for several other proteins, mostly associated with β-turns [17,66]. Accordingly, metal-binding region (not entirely hidden inside the structure of protein) could easily accessible for metal exchange and may involve small but unique structural rearrangements.

Metal gel-shift and MS data

The pre-requisite for successful application of any mass spectrometry technique while studying protein-metal interactions is the optimization of suitable method that preserves non-covalent complexes. The MALDI technique has been used previously to study non-covalent protein complexes **(supporting information, Table C in S1 File)** by adjusting the range of parameters in order to preserve the non-covalent interactions during acquisition of spectra [46,47,67].

Using mild-acidic matrix, spectral measurements showed distinct peaks, validating one apo-Hpn peak with six of Hpn-Ni^{2+} complexes. Singly charged species of Hpn in MALDI--TOF-MS might allow detection of a sixth Hpn-Ni^{2+} complex in mild-acidic conditions that not reported in previous studies [4,5]. However, appearance of weaker or non-specific protein-metal complexes due to higher amounts of metal added to protein samples is a limitation of the ionization process in positive mode measurements [17] and this possibility for sixth Hpn-Ni^{2+} complex cannot be excluded. The interfaces of metal ions with histidine-rich peptides have not been investigated so far, perhaps because such peptides are not possible to study with routinely used techniques owing to overlapping signals [68]. Even though MS data alone are not sufficient to interpret the exact mechanism of metal-binding to various sites, these data have revealed the high flexibility (plasticity) of Hpn for Ni^{2+} binding and its potential to load higher amounts of Ni^{2+} in such a small structure of ~7 kDa.

Our MS data imply several key points that are complementary to "metal gel-shift". At first, all available Hpn molecules were in metalated form at higher Ni^{2+} in MS data. Similarly, presence of only "metal-gel shift" band at higher Ni^{2+} was observed on SDS-PAGE (Fig 3B). Second, Hpn showed MS peaks for metalated species even treated with lower metal concentrations (Fig 6). This coincides with the appearance of "metal-gel shift" band in all protein-metal molar ratios (lower to higher) on SDS-PAGE (Fig 3B and 3C). Third, mass spectral intensity for apo-Hpn gradually decreased in Ni^{2+}-treated Hpn and subsequently mass spectral intensity for either of the metalated species was increased in respective measurements showing progressive appearance of Hpn-Ni^{2+} peaks. This is also consistent with the gradual increase in heterogeneity of apo-Hpn band followed by compact "metal-gel shift" band.

Interestingly, at relatively higher amount of Ni^{2+}, distribution of mass for each Hpn-Ni^{2+} complex was highly heterogeneous in MS data but on contrary, SDS-PAGE showed only one compact protein band. Electrophoretic separation of metalated species having smaller mass difference of each added Ni^{2+} (0.055 kDa) cannot be distinguished on regular SDS-PAGE owing to limited resolution. Also, several factors can affect the migration of each metalated species of Hpn on SDS-PAGE including consequence of boiling, Laemmli buffer components, re-arrangement of protein-protein, protein-metal, and/or protein-SDS interactions. But this is not the case in MS measurements. In addition, differential ionization efficiency and ion suppression effect in MS may interfere in mass-to-charge ratio [69]. The thermodynamic structures of the apo-protein for metalation and the fully metalated protein for demetalation may not be the same [17]. Thus, without further structural studies, it is intricate to compare precise mass distribution of metalated species on SDS-PAGE and further studies are under investigation. Nevertheless, "metal-gel shift" together with MALDI-TOF-MS data establishes that the positional shift is directly associated with metal-binding to Hpn and it is reversible upon metal removal.

The investigation of "gel shifting" anomaly is important because of the universal use of SDS-PAGE technique, and also for the reason that anomalous migration is observed in almost all the studied histidine-rich proteins. Protein-surfactant interactions are central to the detergent industry, and hence further research of Hpn-SDS-metal ion interactions may help to explore novel insights into the mechanism of SDS-resistance, especially kinetics of obdurate Hpn-metal complexes. Also, considering Ni^{2+}-binding properties of Hpn, such a robust protein can be employed as a potential candidate for Ni^{2+} remediation. In brief, our study reveals a novel mechanism of "metal gel-shift" responsible for shifts in electrophoretic gel mobility of Ni^{2+}-treated Hpn on SDS-PAGE signifying metal-induced conformational changes. This property can be used to explore interactions between histidine-rich proteins and surfactant to investigate how metal-binding to a histidine-rich protein changes its confirmation and hydrophobic or electrostatic interactions.

Supporting information

S1 File. Complementary data about DNA purification from *H. pylori* strain SS1, protocol followed for ELISA analysis and its results, supporting figures and tables along with references are provided.
(PDF)

Acknowledgments

The protocol and facility to perform ELISA was kindly provided by Dr. T. Tsuboi and Dr. E. Takashima (Division of Malaria Research, Proteo-Science Center, Ehime University, Matsuyama, Ehime, Japan).

Author Contributions

Conceptualization: HH EHM.

Formal analysis: RMS.

Investigation: RMS YI JM.

Methodology: RMS HH.

Project administration: HH.

Resources: HH EHM.

Supervision: HH.

Validation: RMS.

Visualization: RMS.

Writing – original draft: RMS.

Writing – review & editing: RMS YI JM EHM HH.

References

1. de Reuse H, Vinella D, Cavazza C. Common themes and unique proteins for the uptake and trafficking of nickel, a metal essential for the virulence of Helicobacter pylori. Front Cell Infect Microbiol. 2013; 3: 1–6.
2. Gilbert JV, Ramakrishna J, Sunderman FW, Wright A, Plaut AG. Protein Hpn: Cloning and characterization of a histidine-rich metal-binding polypeptide in Helicobacter pylori and Helicobacter mustelae. 1995; 63: 2682–2688. PMID: 7790085
3. Ge R, Watt RM, Sun X, Tanner J a, He Q-Y, Huang J-D, et al. Expression and characterization of a histidine-rich protein, Hpn: potential for Ni2+ storage in Helicobacter pylori. Biochem J. 2006; 393: 285–93. doi: 10.1042/BJ20051160 PMID: 16164421
4. Ge R, Zhang Y, Sun X, Watt RM, He Q-Y, Huang J-D, et al. Thermodynamic and kinetic aspects of metal binding to the histidine-rich protein, Hpn. J Am Chem Soc. 2006; 128: 11330–1. doi: 10.1021/ja062589t PMID: 16939237
5. Wegner SV, Ertem E, Sunbul M, He C. Metal-binding properties of Hpn from Helicobacter pylori and implications for the therapeutic activity of bismuth. Chem Sci. 2011; 2: 451.
6. Mobley HL, Garner RM, Chippendale GR, Gilbert JV, Kane AV, Plaut AG. Role of Hpn and NixA of Helicobacter pylori in susceptibility and resistance to bismuth and other metal ions. Helicobacter. 1999; 4: 162–169. PMID: 10469190
7. Seshadri S, Benoit SL, Maier RJ. Roles of His-rich Hpn and Hpn-like proteins in Helicobacter pylori nickel physiology. J Bacteriol. 2007; 189: 4120–6. doi: 10.1128/JB.01245-06 PMID: 17384182
8. Witkowska D, Politano R, Rowinska-Zyrek M, Guerrini R, Remelli M, Kozlowski H. The coordination of NiII and CuII ions to the polyhistidyl motif of Hpn protein: Is it as strong as we think? Chem—A Eur J. 2012; 18: 11088–11099.
9. Chiera NM, Rowinska-Zyrek M, Wieczorek R, Guerrini R, Witkowska D, Remelli M, et al. Unexpected impact of the number of glutamine residues on metal complex stability. Metallomics. 2013; 5: 214–21. doi: 10.1039/c3mt20166j PMID: 23370132
10. Rowinska-Zyrek M, Witkowska D, Bielinska S, Kamysz W, Kozlowski H. The -Cys-Cys- motif in Helicobacter pylori's Hpn and HspA proteins is an essential anchoring site for metal ions. Dalton Trans. 2011; 40: 5604–10. doi: 10.1039/c1dt10187k PMID: 21503353
11. Vinella D, Fischer F, Vorontsov E, Gallaud J, Malosse C, Michel V, et al. Evolution of Helicobacter: Acquisition by gastric species of two histidine-rich proteins essential for colonization. PLoS Pathog. 2015; 11: 1–32.
12. Brayman TG, Hausinger RP. Purification, characterization, and functional analysis of a truncated Klebsiella aerogenes UreE urease accessory protein lacking the histidine-rich carboxyl terminus. J Bacteriol. 1996; 178: 5410–6. PMCID: PMC178359 PMID: 8808929

13. Chan K-H, Li T, Wong C-O, Wong K-B. Structural Basis for GTP-dependent dimerization of hydrogenase maturation factor HypB. PLoS One. 2012; 7: e30547. doi: 10.1371/journal.pone.0030547 PMID: 22276211
14. Fu C, Olson JW, Maier RJ. HypB protein of Bradyrhizobium japonicum is a metal-binding GTPase capable of binding 18 divalent nickel ions per dimer. Proc Natl Acad Sci U S A. 1995; 92: 2333–2337. PMID: 7892266
15. Rey L, Imperial J, Palacios JM, Ruiz-Argüeso T. Purification of Rhizobium leguminosarum HypB, a nickel-binding protein required for hydrogenase synthesis. J Bacteriol. 1994; 176: 6066–6073. PMID: 7928968
16. Hottenrott S, Schumann T, Plückthun a, Fischer G, Rahfeld JU. The Escherichia coli SlyD is a metal ion-regulated peptidyl-prolyl cis/trans-isomerase. J Biol Chem. 1997; 272: 15697–701. PMID: 9188461
17. Kaluarachchi H, Sutherland DE, Young A, Pickering IJ, Stillman MJ, Zamble DB. The Ni(II)-binding properties of the metallochaperone SlyD. J Am Chem Soc. 2009; 131: 18489–18500. doi: 10.1021/ja9081765 PMID: 19947632
18. Jeon WB, Cheng J, Ludden PW. Purification and characterization of membrane-associated CooC protein and its functional role in the insertion of nickel into carbon monoxide dehydrogenase from Rhodospirillum rubrum. J Biol Chem. 2001; 276: 38602–38609. doi: 10.1074/jbc.M104945200 PMID: 11507093
19. Rath A, Glibowicka M, Nadeau VG, Chen G, Deber CM. Detergent binding explains anomalous SDS-PAGE migration of membrane proteins. Proc Natl Acad Sci U S A. 2009; 106: 1760–1765. doi: 10.1073/pnas.0813167106 PMID: 19181854
20. Shi Y, Mowery R a., Ashley J, Hentz M, Ramirez AJ, Bilgicer B, et al. Abnormal SDS-PAGE migration of cytosolic proteins can identify domains and mechanisms that control surfactant binding. Protein Sci. 2012; 21: 1197–1209. doi: 10.1002/pro.2107 PMID: 22692797
21. Tulumello DV, Deber CM. Positions of polar amino acids alter interactions between transmembrane segments and detergents. Biochemistry. 2011; 50: 3928–3935. doi: 10.1021/bi200238g PMID: 21473646
22. Karch CM, Borchelt DR. Aggregation modulating elements in mutant human superoxide dismutase 1. Arch Biochem Biophys. Elsevier Inc.; 2010; 503: 175–82. doi: 10.1016/j.abb.2010.07.027 PMID: 20682279
23. Cun S, Li H, Ge R, Lin MCM, Sun H. A Histidine-rich and Cysteine-rich Metal-binding Domain at the C Terminus of Heat Shock Protein A from Helicobacter pylori: Implication for nickel homeostasis and bismuth susceptibility. J Biol Chem. 2008; 283: 15142–15151. doi: 10.1074/jbc.M800591200 PMID: 18364351
24. Panayotatos N, Radziejewska E, Acheson A, Pearsall D, Thadani A, Wong V. Exchange of a single amino acid interconverts the specific activity and gel mobility of human and rat ciliary neurotrophic factors. J Biol Chem. 1993; 268: 19000–3. PMID: 8395524
25. Hayward LJ. Decreased metallation and activity in subsets of mutant superoxide dismutases associated with familial amyotrophic lateral sclerosis. J Biol Chem. 2002; 277: 15923–15931. doi: 10.1074/jbc.M112087200 PMID: 11854284
26. Saha S, Biswas KH, Kondapalli C, Isloor N, Visweswariah SS. The Linker Region in Receptor Guanylyl Cyclases Is a Key Regulatory Module: mutational analysis of guanylyl cyclase C. J Biol Chem. 2009; 284: 27135–27145. doi: 10.1074/jbc.M109.020032 PMID: 19648115
27. Rath A, Cunningham F, Deber CM. Acrylamide concentration determines the direction and magnitude of helical membrane protein gel shifts. Proc Natl Acad Sci U S A. 2013; 110: 15668–73. doi: 10.1073/pnas.1311305110 PMID: 24019476
28. Lee A, Rourke JO, Ungria MCDE, Robertson B, Daskalopoulos G, Dixon MF. A standardized mouse model of Helicobacter pylori infection: introducing the Sydney strain. 1997; 112: 1386–1397. PMID: 9098027
29. Raab A, Pioselli B, Munro C, Thomas-Oates J, Feldmann J. Evaluation of gel electrophoresis conditions for the separation of metal-tagged proteins with subsequent laser ablation ICP-MS detection. Electrophoresis. 2009; 30: 303–314. doi: 10.1002/elps.200800264 PMID: 19204947
30. Sussulini A, Becker JS. Combination of PAGE and LA-ICP-MS as an analytical workflow in metallomics: state of the art, new quantification strategies, advantages and limitations. Metallomics. 2011; 3: 1271. doi: 10.1039/c1mt00116g PMID: 22020804
31. Otzen D. Protein-surfactant interactions: A tale of many states. Biochim Biophys Acta—Proteins Proteomics; 2011; 1814: 562–591.
32. Köhler C, Neuhaus G. Characterisation of calmodulin binding to cyclic nucleotide-gated ion channels from Arabidopsis thaliana. FEBS Lett. 2000; 471: 133–136. PMID: 10767408

33. Damiani E, Margreth A. Subcellular fractionation to junctional sarcoplasmic reticulum and biochemical characterization of 170 kDa Ca(2+)- and low-density- lipoprotein-binding protein in rabbit skeletal muscle. Biochem J. 1991; 277: 825–832. PMID: 1872815

34. Li J, Lee YJ, Assmann SM. Guard Cells Possess a Calcium-Dependent Protein Kinase That Phosphorylates the KAT1 Potassium Channel 1. Plant Physiol. 1998; 116: 785–795. PMID: 9489023

35. Yoon GM, Cho HS, Ha HJ, Liu JR, Lee HP. Characterization of NtCDPK1, a calcium-dependent protein kinase gene in Nicotiana tabacum, and the activity of its encoded protein. Plant Mol Biol. 1999; 39: 991–1001. PMID: 10344204

36. Romeis T, Franz S, Ehlert B, Liese A, Kurth J, Cazale A. Calcium-Dependent Protein Kinase CPK21 Functions in Abiotic Stress Response in Arabidopsis thaliana. 2011; 4. doi: 10.1093/mp/ssq064 PMID: 20978086

37. Akiyama H, Kanai S, Hirano M, Miyasaka H. A novel plasmid recombination mechanism of the marine cyanobacterium Synechococcus sp. PCC7002. DNA Res. 1998; 5: 327–34. PMID: 10048481

38. Yamauchi S, Ueda Y, Matsumoto M, Inoue U, Hayashi H. Distinct features of protein folding by the GroEL system from a psychrophilic bacterium, Colwellia psychrerythraea 34H. Extremophiles. 2012; 16: 871–882. doi: 10.1007/s00792-012-0483-7 PMID: 22996829

39. Laemmli UK. Cleavage of structural proteins during the assembly of the head of bacteriophage T4. Nature; 1970. pp. 680–685.

40. Jin Y, Manabe T. High-efficiency protein extraction from polyacrylamide gels for molecular mass measurement by matrix-assisted laser desorption/ionization-time of flight-mass spectrometry. Electrophoresis. 2005; 26: 1019–1028. doi: 10.1002/elps.200410187 PMID: 15765489

41. Schlosser G, Pocsfalvi G, Malorni A, Puerta A, de Frutos M, Vekey K. Detection of immune complexes by matrix-assisted laser desorption/ionization mass spectrometry. Rapid Commun Mass Spectrom. 2003; 17: 2741–2747. doi: 10.1002/rcm.1239 PMID: 14673821

42. Rom S, Gilad A, Kalifa Y, Konrad Z, Karpasas MM, Goldgur Y, et al. Mapping the DNA- and zinc-binding domains of ASR1 (abscisic acid stress ripening), an abiotic-stress regulated plant specific protein. Biochimie. 2006; 88: 621–628. doi: 10.1016/j.biochi.2005.11.008 PMID: 16387406

43. Mahadev SR, Hayashi H, Ikegami T, Abe S, Morita EH. Improved Protein Overexpression and Purification Strategies for Structural Studies of Cyanobacterial Metal-Responsive Transcription Factor, SmtB from Marine Synechococcus sp. PCC 7002. Protein J. 2013; 32: 626–634. doi: 10.1007/s10930-013-9525-y PMID: 24264463

44. Watanabe Y, Aburatani K, Mizumura T, Sakai M, Muraoka S, Mamegosi S, et al. Novel ELISA for the detection of raw and processed egg using extraction buffer containing a surfactant and a reducing agent. J Immunol Methods. 2005; 300: 115–123. doi: 10.1016/j.jim.2005.02.014 PMID: 15907925

45. Abràmoff MD, Magalhães PJ, Ram SJ. Image processing with imageJ. Biophotonics Int. 2004; 11: 36–41.

46. Strupat K. Molecular Weight Determination of Peptides and Proteins by ESI and MALDI. 2005; 405: 1–36. doi: 10.1016/S0076-6879(05)05001-9 PMID: 16413308

47. Shi R, Munger C, Asinas A, Benoit SL, Miller E, Matte A, et al. Crystal Structures of Apo and Metal-Bound Forms of the UreE Protein from Helicobacter pylori: Role of Multiple Metal Binding Sites,. Biochemistry. 2010; 49: 7080–7088. doi: 10.1021/bi100372h PMID: 20681615

48. Sutherland DEK, Stillman MJ. Noncooperative cadmium(II) binding to human metallothionein 1a. Biochem Biophys Res Commun. 2008; 372: 840–844. doi: 10.1016/j.bbrc.2008.05.142 PMID: 18533113

49. Liao S-M, Du Q-S, Meng J-Z, Pang Z-W, Huang R-B. The multiple roles of histidine in protein interactions. Chem Cent J. 2013; 7: 44. doi: 10.1186/1752-153X-7-44 PMID: 23452343

50. Kolodziejski PJ, Rashid MB, Eissa NT. Intracellular formation of "undisruptable" dimers of inducible nitric oxide synthase. Proc Natl Acad Sci U S A. 2003; 100: 14263–8. doi: 10.1073/pnas.2435290100 PMID: 14614131

51. Atwood CS, Scarpa RC, Huang X, Moir RD, Jones WD, Fairlie DP, et al. Characterization of copper interactions with Alzheimer amyloid?? peptides: Identification of an attomolar-affinity copper binding site on amyloid β 1–42. J Neurochem. 2000; 75: 1219–1233. PMID: 10936205

52. Tham SJ, Chang CD, Huang HJ, Lee YF, Huang TS, Chang CC. Biochemical characterization of an acid phosphatase from thermus thermophilus. Biosci Biotechnol Biochem. 2010; 74: 727–735. doi: 10.1271/bbb.90773 PMID: 20378986

53. Nowakowski AB, Wobig WJ, Petering DH. Native SDS-PAGE: high resolution electrophoretic separation of proteins with retention of native properties including bound metal ions. Metallomics. 2014; 6: 1068–78. doi: 10.1039/c4mt00033a PMID: 24686569

54. Bullis BL, Li X, Rieder C V., Singh DN, Berthiaume LG, Fliegel L. Properties of the Na+/H+ exchanger protein detergent-resistant aggregation and membrane microdistribution. Eur J Biochem. 2002; 269: 4887–4895. PMID: 12354120

55. Pinato O, Musetti C, Farrell NP, Sissi C. Platinum-based drugs and proteins: Reactivity and relevance to DNA adduct formation. J Inorg Biochem. 2013; 122: 27–37. doi: 10.1016/j.jinorgbio.2013.01.007 PMID: 23435290

56. Erickson HP. Size and shape of protein molecules at the nanometer level determined by sedimentation, gel filtration, and electron microscopy. Biol Proced Online. 2009; 11: 32–51. doi: 10.1007/s12575-009-9008-x PMID: 19495910

57. Solis C, Oliver A, Andrade E. PIXE analysis of proteins from a photochemical center. Nucl. Instr. Meth. Phys. Res. Sect. B, 1998; 136: 928–931. Available: http://www.sciencedirect.com/science/article/pii/S0168583X97008963

58. Binet MRB, Ma R, McLeod CW, Poole RK. Detection and characterization of zinc- and cadmium-binding proteins in Escherichia coli by gel electrophoresis and laser ablation-inductively coupled plasma-mass spectrometry. Anal Biochem. 2003; 318: 30–38. PMID: 12782028

59. Gao Y, Chen C, Zhang P, Chai Z, He W, Huang Y. Detection of metalloproteins in human liver cytosol by synchrotron radiation X-ray fluorescence after sodium dodecyl sulphate polyacrylamide gel electrophoresis. Anal Chim Acta. 2003; 485: 131–137.

60. Verbi FM, Arruda SCC, Rodriguez APM, Perez CA, Arruda MAZ. Metal-binding proteins scanning and determination by combining gel electrophoresis, synchrotron radiation X-ray fluorescence and atomic spectrometry. J Biochem Biophys Methods. 2005; 62: 97–109. doi: 10.1016/j.jbbm.2004.09.008 PMID: 15680280

61. Finney L, Chishti Y, Khare T, Giometti C, Levina A, Lay PA, et al. Imaging metals in proteins by combining electrophoresis with rapid X-ray fluorescence mapping. ACS Chem Biol. 2010; 5: 577–587. doi: 10.1021/cb1000263 PMID: 20392082

62. Weseloh G, Kuhbacher M, Bertelsmann H, Ozaslan M, Kyriakopoulos A, Knochel A, et al. Analysis of metal-containing proteins by gel electrophoresis and synchrotron radiation X-ray fluorescence. J Radioanal Nucl Chem. 2004; 259: 473–477.

63. Mena ML, Moreno-Gordaliza E, Moraleja I, Canas B, Gomez-Gomez MM. OFFGEL isoelectric focusing and polyacrylamide gel electrophoresis separation of platinum-binding proteins. J Chromatogr A. 2011; 1218: 1281–1290. doi: 10.1016/j.chroma.2010.12.115 PMID: 21255782

64. Pitt-Rivers R, Impiombato FS. The binding of sodium dodecyl sulphate to various proteins. Biochem J. 1968; 109: 825–830. PMCID: PMC1187034 PMID: 4177067

65. Kleinschmidt JH, Wiener MC, Tamm LK. Outer membrane protein A of E. coli folds into detergent micelles, but not in the presence of monomeric detergent. Protein Sci. 1999; 8: 2065–2071. doi: 10.1110/ps.8.10.2065 PMID: 10548052

66. Chen SH, Chen L, Russell DH. Metal-induced conformational changes of human metallothionein-2A: A combined theoretical and experimental study of metal-free and partially metalated intermediates. J Am Chem Soc. 2014; 136: 9499–9508. doi: 10.1021/ja5047878 PMID: 24918957

67. Chen F, Gülbakan B, Weidmann S, Fagerer SR, Ibáñez AJ, Zenobi R. Applying mass spectrometry to study non-covalent biomolecule complexes. Mass Spectrom Rev. 2007; 26: 223–257.

68. Witkowska D, Politano R, Rowinska-Zyrek M, Guerrini R, Remelli M, Kozlowski H. The coordination of NiII and Cu(II) ions to the polyhistidyl motif of Hpn protein: is it as strong as we think? Chemistry. 2012; 18: 11088–99. doi: 10.1002/chem.201200780 PMID: 22829429

69. Szájli E, Fehér T, Medzihradszky KF. Investigating the quantitative nature of MALDI-TOF MS. Mol Cell Proteomics. 2008; 7: 2410–2418. doi: 10.1074/mcp.M800108-MCP200 PMID: 18653768